Flagella bending affects macroscopic properties of bacterial suspensions

Electronic Supplementary Material

M. Potomkin, M. Tournus, L. Berlyand, I.S. Aranson

1 MMFS - Mathematical Model of Flagellated Swimmer

1.1 Derivation of MMFS

The model is 2D. The swimmer is a rigid elliptic body with an attached elastic beam representing the flagellum (see Fig. 1). The orientation of the swimmer θ_0 is defined as the orientation of the principal axis of the body with respect to horizontal, and the equation for θ_0 is derived from the torque balance:

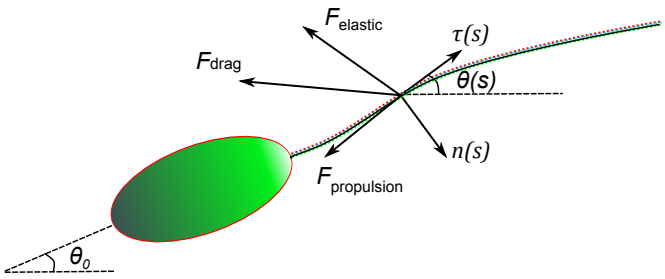

Figure 1:Scheme of flagellated microswimmer

$$\zeta_r \omega = \mathrm{T}_{\mathrm{shear}} + \mathrm{T}_{\mathrm{flagellum}} + \mathrm{T}_{\mathrm{external}}. \quad (1)$$

The equation reads as follows. The viscous torque which is linearly proportional to the angular velocity of the body $\omega = \dfrac{d\theta_0}{dt}$ is balanced by the torques coming from the shear flow, flagellum, and possible external torque (for example, due to the presence of a wall). Equation (1) is a modification of the well-known Jeffery equation for rotating ellipses in a background shear flow [1, 2].

The flagellum is a segment of a curve of the constant length L and with arclength parameter s, $0 \le s \le L$. Unit vectors $\boldsymbol{\tau}(s)$, $\mathrm{n}(s)$ and $\mathbf{b}(s)$ represent tangent, normal and bi-normal vectors of the curve, respectively. Within the flagellum, the viscous (drag) force is balanced by the propulsion and elastic forces:

$$\mathrm{F}_{\mathrm{drag}}(s) = \mathrm{F}_{\mathrm{propulsion}}(s) + \mathrm{F}_{\mathrm{elastic}}(s). \quad (2)$$

The propulsion force is assumed to have a constant magnitude and to be always exerted in the tangent direction: $\mathrm{F}_{\mathrm{propulsion}} = F_p \boldsymbol{\tau}$. The elastic force is given by the internal stress $Q(s)$ which is the force exerted by the segment $[s, L]$ of the flagellum on the segment $[0, s]$. Thus, $\mathrm{F}_{\mathrm{elastic}} = -\dfrac{\partial Q}{\partial s}$. Elasticity of the flagellum is constituted through the relation for internal torque $\mathbf{M}(s) = \boldsymbol{\tau}(s) \times \mathrm{F}_{\mathrm{elastic}}(s)$:

$$\mathbf{M}(s) = K_b \kappa(s) \mathbf{b}(s), \quad (3)$$

where κ is the flagellum curvature. One end, $s = 0$, is rigidly attached to the body (clamped), and another end, $s = L$, of the flagellum is straight and free: $Q(L) = \kappa(L) = 0$.

The propulsion is transmitted to the body, thus, pushing the swimmer forward, through the point of junction and is present in the force balance equation for the body

$$\zeta_b V = \mathrm{F}_{\mathrm{propulsion}}(0) + \mathrm{F}_{\mathrm{elastic}}(0), \tag{4}$$

where $\zeta_b V$ is the drag force for the body.

After proper rewriting, all the above equations (1), (2), (3), (4) result in a coupled system of an ordinary differential equation for the body, a nonlinear elliptic partial differential equation of the second order for the tangential component of Q, a highly nonlinear parabolic partial differential equation of fourth order for the shape of the flagellum, and certain boundary conditions. The system is written in the next subsection of this electronic supplementary material.

1.2 Computation of Trajectories

In this supplementary subsection, we explain how the trajectory of the swimmer and the dynamics of its flagellum are computed in the framework of MMFS. As mentioned before, the swimmer consists of a rigid body and a flexible flagellum (see Fig. 1). The body is an ellipse centered at $X^b(t) = (x^b(t), y^b(t))$ with the major and minor axes ℓ and d, respectively. The swimmer swims in the background flow u^{BG} (either the shear flow $u^{\mathrm{BG}}(x, y) = (-\dot{\gamma}y, 0)$ or zero flow $u^{\mathrm{BG}} = (0, 0)$). The body velocity $V^b(t) = \dfrac{\mathrm{d}X^b(t)}{\mathrm{d}t}$ is given by

$$V^b(t) = u^{\mathrm{BG}}(X^b(t)) + \frac{1}{\zeta_b}\left\{\Lambda(0)\boldsymbol{\tau} + \frac{1}{\alpha}N(0)\mathrm{n}\right\}. \tag{5}$$

Equation (5) reads as follows: relative velocity of the body with respect to background flow is determined by the force exerted by the flagellum (Stokes law); the parameter α takes into account that the ability of the flagellum to drag the body (or, the ability to affect the body velocity) in normal and tangent directions are different, $\alpha \neq 1$. Recall that $Q(s) = \Lambda(s)\boldsymbol{\tau} + N(s)\mathrm{n}$ is the elastic stress, that is the force exerted by the segment $[s, L]$ of the flagellum on the segment $[0, s]$.

The flagellum location $X(s, t) = (x(s, t), y(s, t))$ as a function of the body location $X^b(t) = (x^b(t), y^b(t))$ and flagellum orientation $\theta(s, t)$ is given by the geometrical relations

$$\begin{cases} x(s,t) = x(0,t) + \displaystyle\int_0^s \cos(\theta(z,t))dz, \quad y(s,t) = y(0,t) + \int_0^s \sin(\theta(z,t))dz, \\ x(0,t) = x^b(t) + \dfrac{\ell}{2}\cos(\theta_0(t)), \quad y(0,t) = y^b(t) + \dfrac{\ell}{2}\sin(\theta_0(t)). \end{cases} \tag{6}$$

In order to find $\theta(s, t)$, $\theta_0(t)$, $\Lambda(s, t)$ and $N(s, t)$, the following PDE/ODE system is considered. It consists of an ODE for body orientation angle $\theta_0(t)$, a parabolic forth-order PDE for flagellum orientation angle $\theta(s, t)$, and an elliptic second order PDE for the tangential elastic stress $\Lambda(s, t)$. Independent variables are $t > 0$ and $0 < s < L$.

$$\frac{d\theta_0}{dt} = -\dot{\gamma}\left((1-\beta)\sin^2\theta_0 + \beta\cos^2\theta_0\right) + \frac{\ell}{2\zeta_r}N(0,t), \tag{7}$$

$$\frac{\partial\theta}{\partial t} = -\frac{K_b}{\alpha\zeta_f}\frac{\partial^4\theta}{\partial s^4} + \frac{1}{\zeta_f}\left(\frac{1}{\alpha}\Lambda + K_b\left(\frac{\partial\theta}{\partial s}\right)^2\right)\frac{\partial^2\theta}{\partial s^2} + \frac{1}{\zeta_f}\left(\frac{\alpha+1}{\alpha}\frac{\partial\Lambda}{\partial s} + F_p\right)\frac{\partial\theta}{\partial s} - \dot{\gamma}\sin^2(\theta), \tag{8}$$

$$\frac{\partial^2\Lambda}{\partial s^2} = \frac{1}{\alpha}\left(\frac{\partial\theta}{\partial s}\right)^2\Lambda - K_b\left(\frac{\partial^2\theta}{\partial s^2}\right)^2 - \frac{\dot{\gamma}\zeta_f}{2}\sin(2\theta) - \frac{(\alpha+1)}{\alpha}K_b\frac{\partial^3\theta}{\partial s^3}\frac{\partial\theta}{\partial s}. \tag{9}$$

The system is supplemented with an expression for the normal component of internal stress

$$N = -K_b \frac{\partial^2 \theta}{\partial s^2}, \quad 0 \le s \le L,\ t > 0.$$

The system is also endowed with boundary conditions at $s = 0$ (interface body/flagellum):

$$\theta|_{s=0} = \theta_0, \tag{10}$$

$$\frac{1}{\zeta_b}\Lambda|_{s=0} = \frac{\alpha \ell}{4}\sin(2\theta_0) + \frac{1}{\zeta_f}\left[\frac{\partial \Lambda}{\partial s}|_{s=0} + F_p + K_b \frac{\partial \theta}{\partial s}|_{s=0}\frac{\partial^2 \theta}{\partial s^2}|_{s=0}\right], \tag{11}$$

$$-\left(\frac{1}{\alpha\zeta_b} + \frac{\ell^2}{4\zeta_r}\right) K_b \frac{\partial^2 \theta}{\partial s^2}|_{s=0} = \frac{\beta\dot{\gamma}\ell}{2}\cos(2\theta_0) + \frac{1}{\alpha\zeta_f}\left[-K_b \frac{\partial^3 \theta}{\partial s^3}|_{s=0} + \frac{\partial \theta}{\partial s}\Lambda|_{s=0}\right], \tag{12}$$

and at $s = L$ (free end of the flagellum):

$$\frac{\partial \theta}{\partial s}|_{s=L} = \frac{\partial^2 \theta}{\partial s^2}|_{s=L} = \Lambda|_{s=L} = 0. \tag{13}$$

Remark: We explain now all the drag coefficients appearing in the system above: ζ_b, ζ_f, ζ_r, and α. To drag the elliptic body with the given velocity V and angular velocity ω one need to exert the force $\zeta_b V$ and the torque $\zeta_r \omega$, respectively. It can be shown for ellipses that the drag coefficients ζ_b and ζ_r are related through the following expression:

$$\zeta_r = \frac{\ell^2}{6}\zeta_b. \tag{14}$$

To drag an infinitesimal (small) piece of the flagellum of length Δs with velocity $V_{\boldsymbol{\tau}}\boldsymbol{\tau} + V_{\mathrm{n}}\mathrm{n}$ one needs to exert the drag force $\zeta_f \Delta s\,(\alpha V_{\boldsymbol{\tau}}\boldsymbol{\tau} + V_{\mathrm{n}}\mathrm{n})$. As it is was mentioned above, the parameter α takes into account that drag coefficients in normal and tangent directions are different for the flagellum.

2 Results of Two Scale Asymptotic Expansions

2.1 Original PDE system non-dimensionalized

After the non-dimensionalization

$$\tilde{s} = \frac{s}{L}, \quad \tilde{t} = \dot{\gamma} t, \quad \tilde{\Lambda} = \frac{\Lambda}{\zeta_f \dot{\gamma} L^2}$$

we obtain the following PDE system of MMFS with $t > 0$ and $0 < s < 1$:

$$\begin{cases} \dfrac{d\theta_0}{dt} = -\left((1-\beta)\sin^2\theta_0 + \beta\cos^2\theta_0\right) + \dfrac{3k_r}{r}N_0, & (15) \\ \dfrac{\partial \theta}{\partial t} = -\dfrac{1}{\varepsilon\alpha}\dfrac{\partial^4 \theta}{\partial s^4} + \left(\dfrac{1}{\alpha}\Lambda + \dfrac{1}{\varepsilon}\left(\dfrac{\partial \theta}{\partial s}\right)^2\right)\dfrac{\partial^2 \theta}{\partial s^2} + \left(\dfrac{\alpha+1}{\alpha}\dfrac{\partial \Lambda}{\partial s} + f_p\right)\dfrac{\partial \theta}{\partial s} - \sin^2(\theta), & (16) \\ \dfrac{\partial^2 \Lambda}{\partial s^2} = \dfrac{1}{\alpha}\left(\dfrac{\partial \theta}{\partial s}\right)^2 \Lambda - \dfrac{1}{\varepsilon}\left(\dfrac{\partial^2 \theta}{\partial s^2}\right)^2 - \dfrac{1}{2}\sin(2\theta) - \dfrac{(\alpha+1)}{\alpha\varepsilon}\dfrac{\partial^3 \theta}{\partial s^3}\dfrac{\partial \theta}{\partial s}, & (17) \end{cases}$$

where we dropped tildes in notations for s, t, and Λ, as well as introduce the additional parameters:

$$\varepsilon = \frac{\zeta_f \dot{\gamma} L^4}{K_b}, \qquad f_p = \frac{F_p}{\zeta_f \dot{\gamma} L}, \qquad k_r = \frac{L\zeta_f}{\zeta_b}, \qquad r = \frac{\ell}{L}.$$

In what follows, we obtain asymptotic formulas in the limit $\varepsilon \to 0$.

Equations at $s = 0$:

$$\begin{cases} N_0 = -\dfrac{1}{\varepsilon}\,\dfrac{\partial^2\theta}{\partial s^2}|_{s=0}, \quad \theta|_{s=0} = \theta_0, & (18)\\ k_r\Lambda|_{s=0} = \dfrac{\alpha\, r}{4}\sin(2\theta_0) + \dfrac{\partial\Lambda}{\partial s}|_{s=0} + f_p - \dfrac{\partial\theta}{\partial s}|_{s=0}N_0, & (19)\\ \sigma k_r N_0 = \beta\dfrac{\alpha\, r}{2}\cos(2\theta_0) - \dfrac{1}{\varepsilon}\,\dfrac{\partial^3\theta}{\partial s^3}|_{s=0} + \dfrac{\partial\theta}{\partial s}|_{s=0}\Lambda|_{s=0}. & (20) \end{cases}$$

Here $\sigma = 1 + \dfrac{3\alpha}{2}$.

Equations at $s = 1$:

$$\frac{\partial\theta}{\partial s}|_{s=1} = \frac{\partial^2\theta}{\partial s^2}|_{s=1} = \Lambda|_{s=1} = 0. \tag{21}$$

2.2 Multiscale expansion

$$\begin{cases} \theta(s,t,\tau) = \theta^0(s,t,\tau) + \varepsilon\theta^1(s,t,\tau) + ..., \\ \theta_0(t,\tau) = \theta_0^0(t,\tau) + \varepsilon\theta_0^1(t,\tau) + .., \\ \Lambda(s,t,\tau) = \Lambda^0(s,t,\tau) + \varepsilon\Lambda^1(s,t,\tau) + ..., \\ N_0(t,\tau) = N_0^0(t,\tau) + \varepsilon N_0^1(t,\tau) + ..., \end{cases}$$

Here $\tau = \varepsilon t$ (slow time).

2.3 Modified Jeffery Equation for θ_0^0

The equation for θ_0^0 is obtained by collecting all terms at level ε^0 in (15):

$$\frac{\partial\theta_0^0}{\partial t} = -\left((1-\beta)\sin^2\theta_0^0 + \beta\cos^2\theta_0^0\right) + \frac{3k_r}{r}N_0^0 \tag{22}$$

This is not a closed equation for θ_0^0 because of the unknown term $\dfrac{3k_r}{r}N_0^0$ in the equation (22). In order to find this term (in terms of θ_0^0) first note that due to the first equation in (18) we have

$$N_0^0 = -\frac{\partial^2\theta^1}{\partial s^2}|_{s=0}. \tag{23}$$

Next, expanding equation (16) and collecting all terms at ε^{-1} we get

$$0 = -\frac{1}{\alpha}\frac{\partial^4\theta^0}{\partial s^4} + \left(\frac{\partial\theta^0}{\partial s}\right)^2\frac{\partial^2\theta^0}{\partial s^2}, \quad 0 < s < 1, \tag{24}$$

To write boundary conditions θ^0 at $s = 0$ collect terms at ε^{-1} in the first equation in (18) and (20):

$$\frac{\partial^2\theta^0}{\partial s^2}|_{s=0} = \frac{\partial^3\theta^0}{\partial s^3}|_{s=0} = 0. \tag{25}$$

Equations in (21) give boundary conditions for θ^0 at $s = 1$:

$$\frac{\partial\theta^0}{\partial s}|_{s=1} = \frac{\partial^2\theta^0}{\partial s^2}|_{s=1} = 0. \tag{26}$$

Thus, θ^0 does not depend on s and $\theta^0(s,t,\tau) = \theta_0^0(t,\tau)$:

$$\frac{\partial^i\theta^0}{\partial s^i} \equiv 0, \quad i = 1,2,3,... \tag{27}$$

Due to (27), the equation for θ^1, which is obtained by collecting all terms at ε^0, can be written as

$$\frac{\partial^4\theta^1}{\partial s^4} = \underbrace{-\alpha\left(\frac{\partial\theta_0^0}{\partial t} + \sin^2\theta_0^0\right)}_{=:\chi} \tag{28}$$

Thus, taking into account (21) we obtain

$$\frac{\partial^3\theta^1}{\partial s^3} = \chi\cdot(s-1) + C_1, \tag{29}$$

$$\frac{\partial^2\theta^1}{\partial s^2} = \frac{1}{2}\chi\cdot(s-1)^2 + C_1\cdot(s-1), \tag{30}$$

Here C_1 may depend on t and τ, but not on s. In order to find C_1, use (23), (27) to substitute (29) and (30) with $s=0$ into (20) at level ε^0:

$$C_1 = \frac{\sigma k_r + 2}{2(\sigma k_r+1)}\chi + \frac{\beta\alpha\, r}{2(\sigma k_r+1)}\cos(2\theta_0^0). \tag{31}$$

Now we are in position to find the unknown term in the equation (22):

$$\begin{aligned}\frac{3k_r}{r}N_0^0 &= -\frac{3k_r}{r}\frac{\partial^2\theta^1}{\partial s^2}|_{s=0} = \frac{3k_r}{2r}(-\chi + 2C_1)\\ &= \frac{3k_r}{2r(\sigma k_r+1)}(\chi + \beta\alpha\, r\,\cos(2\theta_0^0))\\ &= -\frac{3\alpha k_r}{2r(\sigma k_r+1)}\left\{\frac{\partial\theta_0^0}{\partial t} + \sin^2\theta_0^0\right\} + \frac{3\beta\alpha k_r}{2(\sigma k_r+1)}\cos 2\theta_0^0.\end{aligned} \tag{32}$$

In order substitute (32) into (22) we note that due to a simple trigonometric identity

$$-\sin^2\theta_0^0 - B\cos(2\theta_0^0) = -(1-B)\sin^2\theta_0^0 - B\cos^2\theta_0^0, \tag{33}$$

with $B=\beta$, the equation (22) can be written as follows:

$$\frac{\partial\theta_0^0}{\partial t} + \sin^2\theta_0^0 = -\beta\cos 2\theta_0^0 + \frac{3k_r}{r}N_0^0. \tag{34}$$

Use (32) to write (34) in the form

$$\left[1 + \frac{3\alpha k_r}{2r(\sigma k_r+1)}\right]\left\{\frac{\partial\theta_0^0}{\partial t} + \sin^2\theta_0^0\right\} = -\beta\left[1 - \frac{3\alpha k_r}{2(\sigma k_r+1)}\right]\cos(2\theta_0^0),$$

or if one divides by $1 + 3\alpha k_r/(2r(\sigma k_r+1))$ and uses identity (33) for

$$B = b := \beta r\frac{2\sigma k_r + 2 - 3\alpha k_r}{2r\sigma k_r + 2r + 3\alpha k_r}, \tag{35}$$

then

$$\frac{\partial\theta_0^0}{\partial t} + \sin^2(\theta_0^0) = -b\cos(2\theta_0^0), \tag{36}$$

or, equivalently,

$$\frac{\partial\theta_0^0}{\partial t} = -(1-b)\sin^2\theta_0^0 - b\cos^2\theta_0^0. \tag{37}$$

The equation (37) has the form of the Jeffery equation, and the main conclusion here is that in the limit of the rigid flagellum $K_b\to\infty$ (equivalently, $\varepsilon\to 0$), the swimmer with the body shape parameter β behaves as the ellipse with no flagellum and with the shape parameter b defined in (35) in place of β.

We note that for typical values of parameters σ, k_r, and α, the parameter b introduced in (35) can be computed by

$$b = \frac{r\beta}{1+2r}.$$

2.4 Asymptotic formula for elastic stress Q

In this subsection we find asymptotic formula for elastic stress $Q^0(t,\tau,s)$, whose the normal and tangential components are N^0 and Λ^0, respectively. The super-index 0 means that we search for values as $\varepsilon \to 0$.

To find N^0 we first note that the equality (23) holds for all $0 \le s \le 1$ (not only for $s = 0$ as in (23)):

$$N^0 = -\frac{\partial^2 \theta^1}{\partial s^2}, \quad 0 \le s \le 1. \tag{38}$$

From (28), (31) and (36) we can easily get

$$\chi = \alpha b \cos(2\theta_0) \quad \text{and} \quad C_1 = \sigma_1 \cos(2\theta_0^0), \tag{39}$$

where

$$\sigma_1 := \frac{\alpha b(\sigma k_r + 2) + \alpha\beta r}{2(\sigma k_r + 1)} \tag{40}$$

Thus, from (30), (38) and (39) it follows that

$$N_0 = -\left(\frac{\alpha b}{2}(s-1)^2 + \sigma_1(s-1)\right)\cos(2\theta_0^0). \tag{41}$$

In order to find Λ^0, we collect all terms at level ε^0 in the equation (17) using (27):

$$\frac{\partial^2 \Lambda^0}{\partial s^2} = -\frac{1}{2}\sin(2\theta_0^0). \tag{42}$$

In view of (21) (a boundary condition at $s = 1$) and that θ_0^0 is independent from s we have

$$\Lambda^0 = -\frac{1}{4}(s-1)^2 \sin 2\theta_0^0 + C_2(s-1). \tag{43}$$

In order to find C_2 use (19):

$$-\frac{k_r}{4}\sin 2\theta_0^0 - k_r C_2 = \frac{\alpha\ r}{4}\sin 2\theta_0^0 + \frac{1}{2}\sin 2\theta_0^0 + C_2 + f_p. \tag{44}$$

Thus,

$$C_2 = -\sigma_2 \sin 2\theta_0^0 - \frac{F_p}{1+k_r}, \quad \text{where} \quad \sigma_2 := \frac{k_r + \alpha r + 2}{4(1+k_r)}. \tag{45}$$

In particular,

$$\Lambda^0 = \left(-\frac{1}{4}(s-1)^2 - \sigma_2(s-1)\right)\sin 2\theta_0^0 - \frac{f_p}{1+k_r}(s-1). \tag{46}$$

Asymptotic formulas for N^0 and Λ^0 in the original scaling:

$$N^0 = -\zeta_f \dot\gamma \left(\frac{\alpha b}{2}(s-L)^2 + L\sigma_1(s-L)\right)\cos 2\theta_0^0. \tag{47}$$

$$\Lambda^0 = -\zeta_f \dot\gamma \left(\frac{1}{4}(s-L)^2 + L\sigma_2(s-L)\right)\sin 2\theta_0^0 - \frac{f_p}{1+k_r}(s-L). \tag{48}$$

2.5 Contribution to effective viscosity

The elastic contribution. From the Kirkwood formula (see Eqn. (2) in the paper) using integration by parts we obtain

$$\eta_{\text{elastic}} = \frac{\Phi}{2\dot{\gamma}\eta_0} \ < \int_0^L (Q\cdot\mathbf{e}_2)\,(\boldsymbol{\tau}\cdot\mathbf{e}_1) + (Q\cdot\mathbf{e}_1)\,(\boldsymbol{\tau}\cdot\mathbf{e}_2)\ ds >_{\theta_0} \tag{49}$$

where $\mathbf{e}_1 = (1,0)$, $\mathbf{e}_2 = (0,1)$, and $< >_{\theta_0}$ denotes the expected value with respect to probability distribution function $P(\theta_0)$ of body orientation angles (see Results section where $P(\theta_0)$ was introduced):

$$< g >_{\theta_0} := \frac{q}{2\pi}\int_0^{2\pi} \frac{g(\theta_0)}{1-(1-2b)\cos(2\theta_0)} d\theta_0, \tag{50}$$

where $q = \sqrt{1-(1-2b)^2}$.

We search for the leading term in ε. Thus, assume $\boldsymbol{\tau} = (\cos\theta, \sin\theta) \approx (\cos\theta_0, \sin\theta_0)$. Then after some straightforward calculations we obtain

$$\eta_{\text{elastic}} = \frac{\Phi}{\dot{\gamma}\eta_0} \ < \int_0^L \Lambda^0(s;\theta_0)\sin 2\theta_0 + N^0(s;\theta_0)\cos(2\theta_0)\ ds >_{\theta_0} \tag{51}$$

Substituting (48) and (47) (with θ_0 instead of θ_0^0) into (51) we get

$$\eta_{\text{elastic}} = \Phi\frac{L^3}{\eta_0} Z_{\text{elastic}}(\beta, r), \tag{52}$$

where

$$\begin{aligned} Z_{\text{elastic}}(\beta,r) = \zeta_f \frac{r\beta}{12(1+2r-2r\beta)}\Big\{&(2r+5)\sqrt{1+2r-r\beta}\Big(2r+1-2\sqrt{r\beta}\sqrt{1+2r-\beta r}\Big) \\ &+ 3\sqrt{r\beta}(3r+2)(2r+1-2\sqrt{r\beta})\Big\}. \end{aligned} \tag{53}$$

The propulsion contribution. The Kirkwood formula for propulsive contribution has the form

$$\begin{aligned} \eta_{\text{propulsion}} &= \frac{\Phi}{2\dot{\gamma}\eta_0} < -F_p \int_0^L (\boldsymbol{\tau}\cdot\mathbf{e}_1)\,(y(s)-y(0)) + (\boldsymbol{\tau}\cdot\mathbf{e}_2)\,(x(s)-x(0))\ ds >_{\theta_0} \\ &= -\frac{F_p\Phi}{2\dot{\gamma}\eta_0} < \int_0^L \int_0^s \cos\theta(s)\sin\theta(w) + \sin\theta(s)\cos\theta(w)\ dw\ ds >_{\theta_0} \end{aligned} \tag{54}$$

Substituting expansion $\theta = \theta^0 + \varepsilon\theta^1 + ...$ into (54) after some cumbersome calculations we obtain

$$\eta_{\text{propulsion}} = -\frac{F_p\Phi}{2\dot{\gamma}\eta_0} < \frac{L^2}{2}\sin(2\theta_0) + \varepsilon L\cos(2\theta_0)\int_0^L \theta^1(s)\ ds >_{\theta_0} + o(\varepsilon). \tag{55}$$

The first term has zero contribution after averaging with respect to θ_0, and the equality (55) becomes

$$\eta_{\text{propulsion}} = -\varepsilon\frac{\Phi F_p L^2}{\eta_0\dot{\gamma}} Z_{\text{prop}}(\beta, r), \tag{56}$$

where

$$Z_{\text{prop}}(\beta, r) = \beta\frac{r(17+10r)(2r+1-q\sqrt{2r+1})}{120(2r+1-\beta r)^2}. \tag{57}$$

3 Estimates for torques due to hydrodynamic interaction with wall and rotation fo helical flagella

There are two main simplifications in the model used to study dynamics of the flagellated swimmer. In these estimates we compare the torque on the body coming from the flagellum bending $\mathrm{T}_{\text{flagellum}}$ with other possible torques which are not taken into account in our model. Recall that we study the impact of the flagellum in two specific situation: when the swimmer is in shear flow and when the swimmer turns at the wall. Note that for a wide range of K_b (namely, $K_b \geq 2.7 \cdot 10^{-24}$ N m^2), if no background flow or obstacle (the wall) is present, then $\mathrm{T}_{\text{flagellum}}$ eventually vanishes and, thus, becomes smaller than the other torques.

The *first* simplification is that we neglect helical structure of the flagellum by considering it as a one-dimensional segment of a curve in a plane. This means that all torques which are taken into account in the model are perpendicular to this plane. On the other hand, it is known that moving bacteria rotate their helical flagella counterclockwise around its major axis as viewed from behind [3]. Thus, an active torque on the body is imposed, and this torque is parallel or almost parallel to this plane. For example, in Ref. [4] a model which takes into account the helical shape of flagellum and its rotation around major axis of the swimmer was considered and the buckling instability of the flagellum was observed. In this paper, we neglect the torque due to the flagellum rotation and still we are able to observe a similar phenomenon (see Fig. 2, (d) where the same type of bifurcation is observed with respect to parameter K_b).

Next we give an estimate for the torque due to rotation of helical flagellum along the swimmer's major axis. We use the formula from Ref. [3]:

$$\mathrm{T}_{\text{axial rotation}} = \omega \left[A \sin^2 \varphi + B \cos^2 \varphi \right], \tag{58}$$

where $\omega = 1.5$ rev s^{-1} is the angular speed of the flagellum rotation, φ is the angle between the body orientation and the flagellum major axis. We assume that $0 \leq \varphi \leq 0.02\pi$ (the angle 0.02π corresponds to planar "wobbling" in our model for $K_b = 2 \cdot 10^{-24}$ N m^2).

Parameters A and B are defined as follows:

$$A = 32\pi\eta\ell d^2 e^3 \frac{2-e^2}{3(1-e^2)(1+e^2)E - 2e} + 28\pi\eta\ell^3 e^3 \frac{1}{(3e^2-1)E + 2e}, \tag{59}$$

$$B = 32\pi\eta\ell d^2 e^3 \frac{1}{3(2e-(1-e^2)E)}, \tag{60}$$

where $e = \dfrac{\sqrt{\ell^2 + d^2}}{\ell}$ and $E = \ln[1+e] - \ln[1-e]$. For these values of parameters we have

$$\mathrm{T}_{\text{axial rotation}} \approx 250 \text{ pN nm} \quad \ll \quad \mathrm{T}_{\text{flagellum}} \approx 7.5 \text{ pN mm}. \tag{61}$$

Here $\mathrm{T}_{\text{flagellum}}$ is the torque due to flagellum bending. The value of $\mathrm{T}_{\text{flagellum}}$ used above corresponds to amplitude of flagellum bending force N_0 for $K_b = 2 \cdot 10^{-24}$ N m^2 which equals to $0.756\zeta_f \dot{\gamma} L$. Thus, the torque due to the helical shape of the flagellum is negligible in compare to the one due to flagellum bending.

The *second* simplification is that we do not consider local effects on the fluid in the swimmer's proximity. This in turn leads to neglecting of hydrodynamic interaction with the wall. To estimate the hydrodynamic torque due to the presence of the wall (note that the torque $\mathrm{T}_{\text{steric-wall}}$ is due to steric interactions between the swimmer's body and the wall) we use the approach from Refs. [5, 6]:

$$\mathrm{T}_{\text{hydrodynamic-wall}} = f_r \, \frac{3V(\ell + L)\sin(2\theta)}{128\pi h^3} \tag{62}$$

$f_r = 1.6 \times 10^{-18}$ N s m is the drag coefficient, $V = 20$ μm s^{-1} is the swimmer's speed, $h = 2$ μm is the distance between the bacterium and the wall (this value is taken from [6]; it is assumed that the

swimmer does not actually touches the surface, otherwise the formula (62) is not applicable due to the h^{-3} term). For these values of parameters and $\sin(2\theta) = 0.1 \ll 1$ (so either $\theta \approx 0$, swimmer is perpendicular to the wall, or $\theta \approx \pm\pi/2$, swimmer is parallel to the wall; for the intermediate angles, between 0 and $\pi/2$, torque $\mathrm{T}_{\text{hydrodynamic-wall}}$ helps to turn the swimmer from the perpendicular entrapment) $\mathrm{T}_{\text{hydrodynamic-wall}} = 10 - 20$ pN μm is much smaller than $\mathrm{T}_{\text{flagellum}} = .1 - .2$ pN mm.

4 Description of videos

Videos S1-S5 are obtained by a numerical solution of the model described in the paper. The parameters values are described on Table 2 at the end of the paper. No external flow is imposed.

Video S1

The swimmer is initially oriented perpendicular to the wall, the initial shape of its flagellum is slightly non-symmetric. Depending on the bending stiffness, the swimmer is eventually either trapped at the wall but keeps oscillating ($K_b = 2{\cdot}10^{-24}$ N m^2, left panel), or escapes the wall ($K_b = 2 \cdot 10^{-23}$ N m^2, center), or trapped at the wall with no visible oscillations ($K_b = 3 \cdot 10^{-23}$ N m^2, right panel).

Videos S2, S3 and S4

For each of the 3 values of K_b ($2 \cdot 10^{-24}$ N m^2, $2 \cdot 10^{-23}$ N m^2, and $3 \cdot 10^{-23}$ N m^2, respectively) picked for Video S1, the swimmer is displayed on a moving frame centered near its body.

Video S5

This video illustrates the two different ways of swimming when no obstacles are present in the fluid. The swimmer swims straight ($K_b = 3 \cdot 10^{-23}$ N m^2, lower panel), or exhibits periodic oscillations ($K_b = 2 \cdot 10^{-24}$ N m^2, upper panel).

References

[1] G. Jeffery, "The Motion of Ellipsoidal Particles Immersed in a Viscous Fluid," *Proceedings of the Royal Society A*, vol. 102, no. 715, pp. 161–179, 1922.

[2] S. Kim and J. Karrila, *Microhydrodynamics: Principles and Selected Applications*. Dover, 1991.

[3] N. Darnton, L. Turner, S. Rojevsky, and H. Berg, "On Torque and Tumbling in Swimming Escherichia coli," *Journal of Bacteriology*, vol. 189, no. 5, pp. 1756–1764, 2007.

[4] R. Vogel and H. Stark, "Motor-driven bacterial flagella and buckling instabilities," *European Physical Journal E: Soft Matter*, vol. 35, no. 15, pp. 1–15, 2012.

[5] A. Berke, L. Turner, H. Berg, and E. Lauga, "Hydrodynamic attraction of swinning microorganisms by surfaces," *Physical Review Letters*, vol. 101, p. 038102, 2008.

[6] P. Mushenheim, R. Trivedi, S. Roy, M. Arnold, D. Weibel, and N. Abbott, "Effects of cofinement, surface-induced orientations and strain on dynamical behaviors of bacteria in thin liquid crystalline films," *Soft Matter*, vol. 11, no. 34, pp. 6821–6831, 2015.